Available online at www.sciencedirect.com
ScienceDirect
Applied Mathematics and Computation 187 (2007) 1351–1367
APPLIED MATHEMATICS AND COMPUTATION
www.elsevier.com/locate/amc

# A numerical study on the finite element solution of singularly perturbed systems of reaction–diffusion problems

C. Xenophontos [a,*], L. Oberbroeckling [b]

[a] Department of Mathematics and Statistics, University of Cyprus, P.O. Box 20537, 1678 Nicosia, Cyprus
[b] Department of Mathematical Sciences, Loyola College, 4501 N. Charles Street, Baltimore, MD 21210, United States

## Abstract

We consider the approximation of singularly perturbed systems of reaction–diffusion problems, with the finite element method. The solution to such problems contains boundary layers which overlap and interact, and the numerical approximation must take this into account in order for the resulting scheme to converge uniformly with respect to the singular perturbation parameters. In this article we conduct a numerical study of several finite element methods applied to a model problem, having as our goal their assessment and the identification of a high order scheme which approximates the solution at an exponential rate of convergence, independently of the singular perturbation parameters.
© 2006 Elsevier Inc. All rights reserved.

*Keywords:* Singularly perturbed system; Boundary layers; Finite element method; *hp* version; Shishkin mesh

## 1. Introduction

The numerical solution of singularly perturbed problems has been studied extensively over the last decade (see, e.g., the books [14,15,17] and the references therein). The main difficulty in these problems is the presence of *boundary layers* in the solution, whose accurate approximation, independently of the singular perturbation parameter(s), is of utmost importance in order for the overall quality of the approximate solution to be good. In the context of the finite element method (FEM), the robust approximation of boundary layers requires either the use of the *h* version on non-uniform meshes (such as the Shishkin mesh [20] or the Bakhvalov mesh [1]), or the use of the high order *p* and *hp* versions on specially designed (variable) meshes [21]. In both cases, the a priori knowledge of the position of the layers is taken into account, and mesh-degree combinations can be chosen for which uniform error estimates can be established [7,21].

In this article we consider a *system* of two coupled singularly perturbed linear reaction–diffusion equations, which have two overlapping boundary layers. This problem was studied by Matthews et al. [11,12], Madden and Stynes [10] and by Linß and Madden [8,9] in the context of finite differences, and by Linß and Madden [7]

* Corresponding author.
*E-mail address:* xenophontos@ucy.ac.cy (C. Xenophontos).

0096-3003/$ - see front matter © 2006 Elsevier Inc. All rights reserved.
doi:10.1016/j.amc.2006.09.044

in the context of the $h$ version of the FEM with piecewise linear basis functions. Here we consider the finite element approximation of the same problem, paying particular attention to the high order versions of the FEM. Our goal is to numerically investigate the performance of all versions of the FEM on various meshes and to identify a method which approximates the solution independently of the singular perturbation parameters at a sufficiently fast rate. In fact, we propose a $p/hp$ FEM on a five element variable mesh which, as our numerical computations will demonstrate, approximates the solution at an *exponential* rate of convergence, independently of the singular perturbation parameters.

The rest of the paper is organized as follows: In Section 2 we present the model problem and discuss the properties of its solution. In Section 3 we give the finite element formulation and the design of the various schemes we will be considering. Section 4 contains the results of extensive numerical computations in order to assess the performance of each method, and finally, in Section 5 we summarize our conclusions.

In what follows, the space of squared integrable functions on an interval $\Omega \subset \mathbb{R}$ will be denoted by $L^2(\Omega)$, with associated inner product

$$(u, v)_\Omega := \int_\Omega uv.$$

We will also utilize the usual Sobolev space notation $H^k(\Omega)$ to denote the space of functions on $\Omega$ with $0, 1, 2, \ldots, k$ generalized derivatives in $L^2(\Omega)$, equipped with norm and seminorm $\|\cdot\|_{\Omega,1}$ and $|\cdot|_{\Omega,1}$, respectively. For vector functions $\vec{u} = [u_1(x), u_2(x)]^{\mathrm{T}}$, we will write

$$\|\vec{u}\|^2_{\Omega,k} = \|u_1\|^2_{\Omega,k} + \|u_2\|^2_{\Omega,k}.$$

We will also use the space

$$H^1_0(\Omega) = \{u \in H^1(\Omega) : u|_{\partial\Omega} = 0\},$$

where $\partial\Omega$ denotes the boundary of $\Omega$. Finally, the letter $C$ will be used to denote a generic positive constant, independent of any discretization or singular perturbation parameters and possibly having different values in each occurrence.

## 2. The model problem

As in [7,8,9,10,11,12], we consider the following model problem: find $\vec{u}$ such that

$$L\vec{u} := \begin{bmatrix} -\varepsilon^2 \frac{d^2}{dx^2} & 0 \\ 0 & -\mu^2 \frac{d^2}{dx^2} \end{bmatrix} \vec{u} + A\vec{u} = \vec{f} \quad \text{in } \Omega = (0,1), \tag{1}$$

along with the boundary conditions on $\partial\Omega$

$$\vec{u}(0) = \vec{\gamma}_0, \quad \vec{u}(1) = \vec{\gamma}_1. \tag{2}$$

In (1) the parameters $\varepsilon$ and $\mu$ lie in $(0, 1]$,

$$A = \begin{bmatrix} a_{11}(x) & a_{12}(x) \\ a_{21}(x) & a_{22}(x) \end{bmatrix}, \quad \vec{f} = \begin{bmatrix} f_1(x) \\ f_2(x) \end{bmatrix} \tag{3}$$

are given, and we will take, without loss of generality, $\vec{\gamma}_0 = \vec{\gamma}_1 = \vec{0}$ in (2). Moreover, we will assume that the matrix $A$ is invertible and that there exists some constant $\alpha$ such that

$$\min_{x\in[0,1]} \{a_{11}(x) + a_{12}(x), a_{21}(x) + a_{22}(x)\} > \alpha^2 > 0. \tag{4}$$

Problems of this type arise in the study of turbulence models [16,22], population dynamics [5], as well as in the modeling of mass transfer processes in multicomponent systems [19]. Moreover, when $\mu = 1$, the system (1) corresponds to the scalar fourth-order singularly perturbed problem studied in [18], hence our study contains this as a special case.

We will concentrate on the most general case (see, e.g., [10]) when

$$0 < \varepsilon \leqslant \mu \leqslant 1,$$

and our goal will be to obtain a finite element approximation for the solution $\vec{u} := [u_1(x), u_2(x)]^T$ to (1), that is valid *uniformly* in $\varepsilon$ and $\mu$, i.e., the method does not deteriorate as $\varepsilon, \mu \to 0$. It is known that in this case the solution $\vec{u}$ will contain boundary layers of width $O(|\mu \ln \mu|)$, but as it was shown in [10], the first component of $\vec{u}$ will contain an additional sublayer of width $O(|\varepsilon \ln \varepsilon|)$. This is demonstrated in Fig. 1, in which the two components of the solution $\vec{u}$ are shown, for the case

$$A = \begin{bmatrix} 2 & -1 \\ -1 & 2 \end{bmatrix}, \quad \vec{f}(x) = \begin{bmatrix} 1 \\ 1 \end{bmatrix}, \quad \vec{u}(0) = \begin{bmatrix} 0 \\ 0 \end{bmatrix}, \quad \varepsilon = 10^{-7}, \quad \mu = 10^{-4}. \tag{5}$$

In [10], it was shown that the solution to (1) and (2) can be decomposed into a smooth part and a boundary layer part, and bounds on each were obtained which allowed for the design of a uniformly (in $\varepsilon$ and $\mu$) convergent finite difference scheme on a Shishkin mesh, to be constructed. These bounds were subsequently utilized in [7] for the design of a piecewise linear finite element scheme (on Shishkin and Bakhvalov meshes), which again was shown to be uniformly convergent. In particular, the results of [10] state that if $\vec{u}$ solves (1), and $\vec{U}$ is the approximation obtained using centered second order finite differences on a Shishkin mesh with nodes $\{x_i\}_{i=0}^N$, then

$$\|\vec{u} - \vec{U}\|_N \leqslant CN^{-1} \ln N, \tag{6}$$

where $\|\vec{u}\|_N = \max_{k=1,2}\{\max_{i=0,\dots,N}|u_k(x_i)|\}$. The above error estimate was improved in [9] where it was shown that the same central difference scheme gives almost second order accuracy (as opposed to almost first order accuracy shown in [10]); see also [8]. A similar error estimate to (6) was also obtained in [7], in terms of the energy norm (see Eq. (12) ahead), with $\vec{U}$ being the piecewise linear finite element approximation on the Shishkin mesh. More details on the finite element approximation of this problem, and the error estimates obtained in [7], will be given in the next section.

An example of the Shishkin mesh used in the articles mentioned above is shown in Fig. 2, in which

$$\tau_\mu = \min\left\{\frac{1}{4}, \frac{\mu}{\alpha} \ln N\right\}, \quad \tau_\varepsilon = \min\left\{\frac{1}{8}, \frac{\tau_\mu}{2}, \frac{\varepsilon}{\alpha} \ln N\right\}. \tag{7}$$

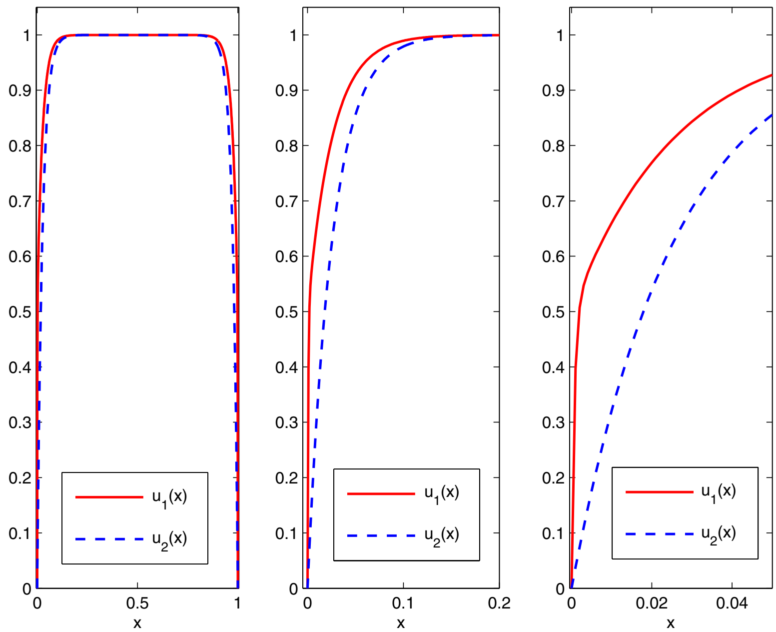


Fig. 1. The exact solution of (1) for the example given by (5).

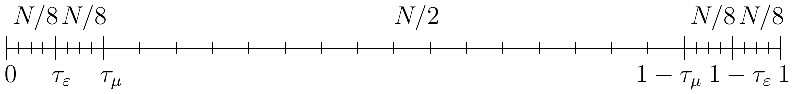


Fig. 2. Example of a Shishkin mesh with $N = 32$ subintervals.

## 3. The finite element methods

As usual, we cast the problem (1) into an equivalent weak formulation, which reads: find $\vec{u} \in [H_0^1(\Omega)]^2$ such that

$$B(\vec{u}, \vec{v}) = F(\vec{v}) \quad \forall \vec{v} \in [H_0^1(\Omega)]^2, \tag{8}$$

where

$$B(\vec{u}, \vec{v}) = \varepsilon^2(u_1', v_1')_\Omega + \mu^2(u_2', v_2')_\Omega + (a_{11}u_1 + a_{12}u_2, v_1)_\Omega + (a_{21}u_1 + a_{22}u_2, v_2)_\Omega, \tag{9}$$

$$F(\vec{v}) = (f_1, v_1)_\Omega + (f_2, v_2)_\Omega. \tag{10}$$

From (4), we get that for any $x \in \Omega$,

$$\vec{\xi}^{\mathrm{T}} A \vec{\xi} \geqslant \alpha^2 \vec{\xi}^{\mathrm{T}} \vec{\xi} \quad \forall \vec{\xi} \in \mathbb{R}^2, \tag{11}$$

and it follows that the bilinear form $B(\cdot,\cdot)$ is coercive with respect to the *energy norm*

$$\|\vec{u}\|_{E,\Omega}^2 := \varepsilon^2 |u_1|_{1,\Omega}^2 + \mu^2 |u_2|_{1,\Omega}^2 + \alpha^2(\|u_1\|_{0,\Omega}^2 + \|u_2\|_{0,\Omega}^2), \tag{12}$$

i.e.,

$$B(\vec{u}, \vec{u}) \geqslant \|\vec{u}\|_{E,\Omega}^2 \quad \forall \vec{u} \in [H_0^1(\Omega)]^2. \tag{13}$$

This, along with the continuity of $B(\cdot,\cdot)$ and $F(\cdot)$, imply the unique solvability of (8).

For the discretization, we choose a finite dimensional subspace $V_N$ of $H_0^1(\Omega)$ and solve the problem: find $\vec{u}_N \in [V_N]^2$ such that

$$B(\vec{u}_N, \vec{v}) = F(\vec{v}) \quad \forall \vec{v} \in [V_N]^2. \tag{14}$$

The unique solvability of the discrete problem (14) follows from (11) and (13). The subspace $V_N$ is chosen as follows. Let $\Delta = \{0 = x_0 < x_1 < \cdots < x_M = 1\}$ be an arbitrary partition of $\Omega = (0,1)$ and set

$$I_j = (x_{j-1}, x_j), \quad h_j = x_j - x_{j-1}, \qquad j = 1, \ldots, M,$$
$$h_{\max} = \max_{j=1,\ldots,M} h_j.$$

Also, define the master (or standard) element $I_{ST} = (-1, 1)$, and note that it can be mapped onto the $j$th element $I_j$ by the linear mapping

$$x = Q_j(t) = \frac{1}{2}(1 - t)x_{j-1} + \frac{1}{2}(1 + t)x_j.$$

The inverse mapping, which maps the $j$th element onto the standard element, is given by

$$t = Q_j^{-1}(x) = \frac{2t - x_{j-1} - x_j}{h_j}.$$

With $\Pi_p(I_{ST})$ the space of polynomials of degree $\leqslant p$ on $I_{ST}$, we define our finite dimensional subspace as

$$V_N \equiv V_N(\Delta, \vec{p}) = \{u \in H_0^1(\Omega) : u(Q_j(t)) \in \Pi_{p_j}(I_{ST}), j = 1, \ldots, M\}, \tag{15}$$

where $\vec{p} = (p_1, \ldots, p_M)$ is the vector of polynomial degrees assigned to the elements. This construction allows us to study all the versions of the FEM, namely: (i) the $h$ version, in which $\vec{p}$ is fixed and $h_{\max} \to 0$, (ii) the $p$ version, in which the mesh (i.e. $h_j$) is fixed and $p_j \to \infty\ \forall j$, and (iii) the $hp$ version, which is a combination of the previous two. We will focus our attention to the design of a high order $p/hp$ FEM on a suitable (variable) mesh, which will approximate the solution to (1) uniformly in $\varepsilon$ and $\mu$, at an *exponential* rate.

The idea for a high order method for singularly perturbed problems comes from the study of the scalar problem

$$-\varepsilon^2 u''(x) + b(x)u(x) = f(x) \quad \text{in } \Omega = (0,1), \tag{16}$$

$$u(0) = u(1) = 0. \tag{17}$$

Schwab and Suri [21] showed that, in the case when $b(x)$ is constant, the use of the three element mesh

$$\Delta = \{0, p\varepsilon, 1 - p\varepsilon, 1\}, \tag{18}$$

in conjunction with the $p$ version of the FEM yields exponential convergence rates, independently of $\varepsilon$, when the error is measured in the energy norm (see also [23]). In (18), the degree $p$ of the approximating polynomials is increased until $\varepsilon p \approx 1$; once $p \approx \varepsilon^{-1}$, we enter the asymptotic range of $p$ and using the $p$ version on a single element yields exponential convergence (see [21] for more details). The non-constant coefficient case of problem (16) was studied by Melenk [13], where the exponential convergence rate was established for any $b$ and $f$ which are analytic.

In terms of the $h$ version of the FEM for problem (16), the use of piecewise polynomials of degree $p$ on a Shishkin mesh with $O(N)$ elements, is known to yield the quasi-optimal algebraic convergence rate $O((N^{-1}\ln N)^p)$ [25]. The optimal algebraic rate $O(N^{-p})$ for the $h$ version can be attained if a Bakhvalov mesh [1], or an exponentially graded mesh is used (cf. [2,3,24]). See also [4] for an alternative approach based on mesh equidistribution which also yields the optimal rate. In [6] yet another scheme on a highly anistropic mesh was presented which yielded results comparable to those based on the Shishkin mesh. For the sake of brevity, we choose to only consider the exponentially graded mesh from [24] from this point forward. For the scalar problem (16) the exponentially graded mesh is defined as $\Delta = \{x_j^\varepsilon\}_{j=0}^N$, where

$$x_j^\varepsilon = \frac{1}{2}\varepsilon(2p+1)\ln\left(1 - \frac{s_j}{N}\right) \quad \text{with } s_j = 1 - \exp\left(-\frac{2}{\varepsilon(2p+1)}\right), \tag{19}$$

and is shown in Fig. 3 (see [24] for more details, including the derivation of (19).)

Guided by the above results for the scalar problem, and the behavior of the overlapping layers for the system (1), we design the following finite element schemes: for the $p/hp$ version, we use the five element variable mesh

$$\Delta = \{0, p\varepsilon, p\mu, 1 - p\mu, 1 - p\varepsilon, 1\}, \tag{20}$$

with $p$ increasing, under the assumptions that $0 < p\varepsilon < p\mu$ and $1 - p\mu < 1 - p\varepsilon < 1$. If $\max\{p\varepsilon, p\mu\} \approx 1$ then we simply use a single element and increase $p$. Moreover, if $\varepsilon = \mu$ or either $\varepsilon$ or $\mu = 1$, then we use the three element mesh (18). As our numerical results in the next section will indicate, this scheme will yield exponential convergence, independently of $\varepsilon$ and $\mu$, and the following error estimate will be observed:

$$\|\vec{u} - \vec{u}_N\|_{E,\Omega} \leqslant C\max\{\varepsilon^{1/2}, \mu^{1/2}\}e^{-\kappa p}, \quad \kappa \in \mathbb{R}^+. \tag{21}$$

(The proof of (21) appears in [26].) For the $h$ version, we will construct an exponentially graded mesh, suitable for the system (1), by taking the union of the meshes obtained using (19); once with $\varepsilon$ and once with $\varepsilon$ replaced by $\mu$, i.e., $\Delta = \{x_j^\varepsilon\}_{j=0}^N \cup \{x_j^\mu\}_{j=0}^N$. As our numerical computations in the next section will indicate, this method will yield the optimal convergence rate $O(N^{-p})$. We will also consider the $h$ version on a Shishkin mesh, with

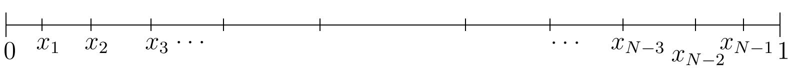


Fig. 3. Example of the exponentially graded mesh with $N = 12$ nodes.

polynomials of degree $p = 1$, 2 and 3. Since the definition of the mesh from [7,10], seen in Fig. 2, corresponds to $p = 1$, we will take

$$\tau_\mu = \min\left\{\frac{1}{4}, \frac{\mu}{\alpha}(p+1)\ln N\right\}, \quad \tau_\varepsilon = \min\left\{\frac{1}{8}, \frac{\tau_\mu}{2}, \frac{\varepsilon}{\alpha}(p+1)\ln N\right\}$$

for our computations, instead of (7).

We close this section by mentioning the error estimates obtained in [7] for the model problems (1) and (2) using the finite element method with piecewise linear basis functions. For the Shishkin mesh, it was shown that

$$\|\vec{u} - \vec{u}_N\|_{E,\Omega} \leqslant C_1 N^{-1} \ln N,$$

and for the Bakhvalov mesh, the following was established:

$$\|\vec{u} - \vec{u}_N\|_{E,\Omega} \leqslant C_2 N^{-1},$$

with the positive constants $C_1$, $C_2$ independent of $N$, $\varepsilon$ and $\mu$. Our computations in the next section will suggest that the above error estimate for the Shishkin mesh can be generalized for polynomials of degree $p \geqslant 1$.

## 4. Numerical results

In this section we present the results of numerical computations for the two model problems considered in [7,10]. Our goal will be to compare the different types of finite element schemes, as well as verify the claims made in Section 3 regarding the high order FEMs and the $h$ version on the exponentially graded mesh. Also, we will present results for the Shishkin mesh with $p = 2$ and 3 (in addition to $p = 1$), which, as mentioned above, suggest that the results in [7] can be generalized.

### 4.1. The constant coefficient case

First we consider the constant coefficient case, in which

$$A = \begin{bmatrix} 2 & -1 \\ -1 & 2 \end{bmatrix}, \quad \vec{f}(x) = \begin{bmatrix} 1 \\ 1 \end{bmatrix}, \quad \vec{u}(0) = \begin{bmatrix} 0 \\ 0 \end{bmatrix}.$$

An exact solution is available, hence the computations we report are reliable. We will be comparing the following methods:

- The $h$ version on a uniform mesh, with $p = 1$, 2 and 3.
- The $p$ version on a single element.
- The $hp$ version on the five element (variable) mesh given by (20).
- The $h$ version on a Shishkin mesh, with $p = 1$, 2 and 3.
- The $h$ version on the exponentially graded mesh given by (19), with $p = 1$, 2 and 3.

We expect that the first two methods will not be robust, while the last three will. We will be plotting the percentage relative error in the energy norm, given by

$$100 \times \frac{\|\vec{u}_{\mathrm{EXACT}} - \vec{u}_{\mathrm{FEM}}\|_{E,\Omega}}{\|\vec{u}_{\mathrm{EXACT}}\|_{E,\Omega}}, \tag{22}$$

versus the number of degrees of freedom $N$, on a log–log scale.

Fig. 4 shows the error when $\varepsilon = 0.4$ and $\mu = 1$. Since these values are "large", we see that the $h$ version on a uniform mesh performs sufficiently well (with $O(N^{-p})$ convergence rate), and the $p$ version on a single element yields exponential convergence.

In Fig. 5, $\varepsilon = 0.01$ and $\mu = 0.1$, and we see the performance of the aforementioned methods beginning to deteriorate, even though the $p$ version still converges exponentially due to the fact that we continue to have $p \approx \varepsilon^{-1}$.

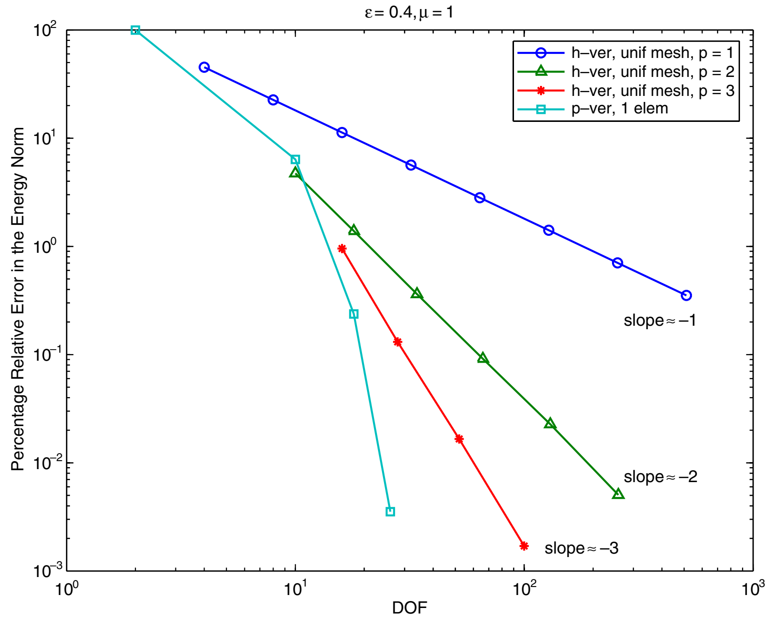


Fig. 4. Energy norm convergence for $\varepsilon = 0.4$ and $\mu = 1$.

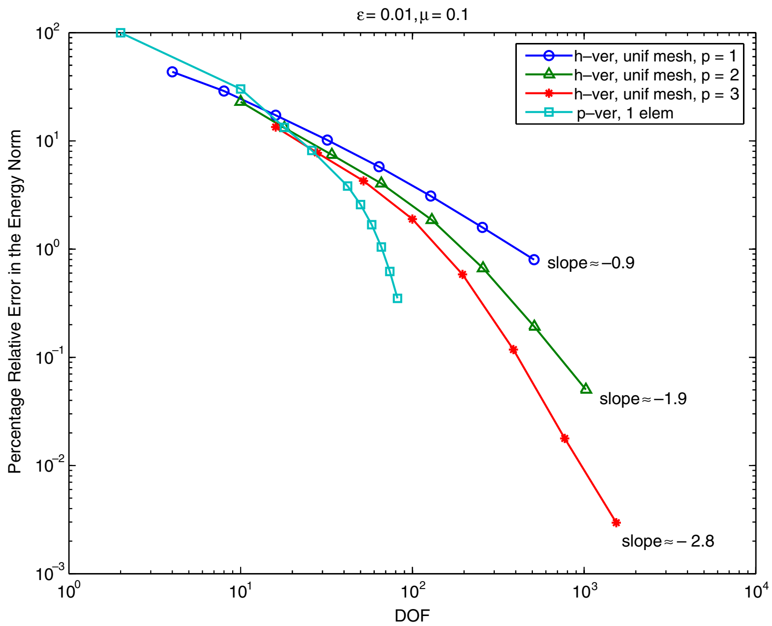


Fig. 5. Energy norm convergence for $\varepsilon = 0.01$ and $\mu = 0.1$.

The deterioration of these methods is seen in Fig. 6 with $\varepsilon = 10^{-7/2} \approx 3 \times 10^{-4}$ and $\mu = 0.01$. We observe that the $h$ version on a uniform mesh converges at the rate $O(N^{-0.7})$, independently of the polynomial degree used, while the $p$ version no longer converges exponentially, but at the algebraic rate $O(N^{-1.5})$ which is roughly twice that of the $h$ version.

For these values of $\varepsilon$ and $\mu$, we show in Fig. 7 the behavior of the $h$ version on the uniform, Shishkin and exponential meshes with $p = 1$, the $p$ version on 1 element and the $hp$ version on five elements. This figure

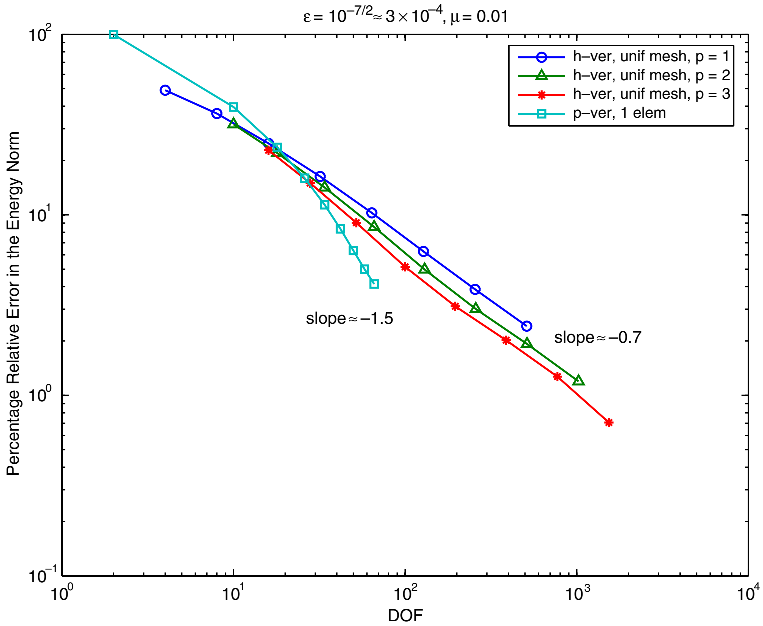


Fig. 6. Energy norm convergence for $\varepsilon = 10^{-7/2} \approx 3 \times 10^{-4}$ and $\mu = 0.01$.

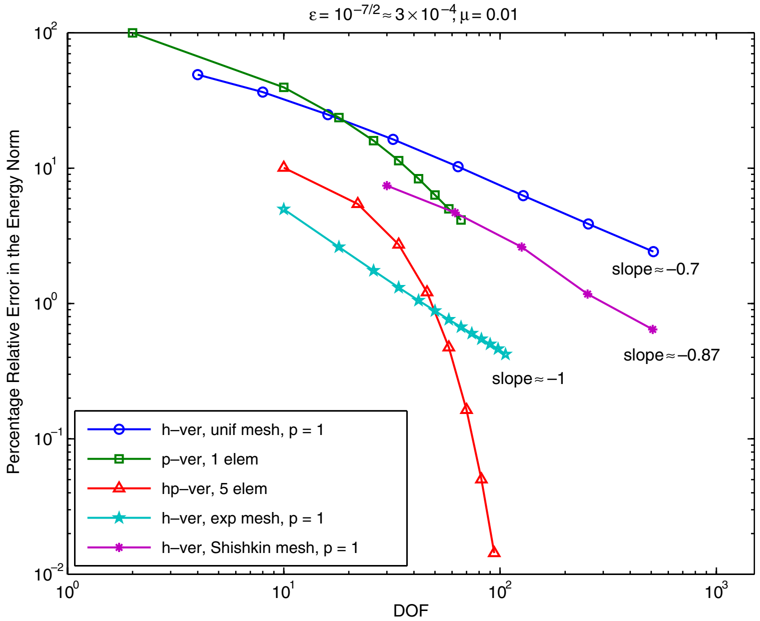


Fig. 7. Energy norm convergence for $\varepsilon = 10^{-7/2} \approx 3 \times 10^{-4}$ and $\mu = 0.01$.

clearly indicates the robustness of the $h$ version on the Shishkin and exponential meshes, as well as the exponential convergence of the $hp$ version on the five element mesh.

Fig. 8 shows the behavior of the robust $h$ versions with different polynomial degrees. We see that the exponential mesh produces the optimal algebraic rate $O(N^{-p})$, while the Shishkin mesh yields the (usual) quasi-optimal rate $O((N^{-1}\ln N)^p)$, with the logarithmic term not removable. For completeness, we have included the $hp$ version to see how it compares with the robust $h$ versions, and we see that only the $h$ version on the exponential mesh is comparable to it.

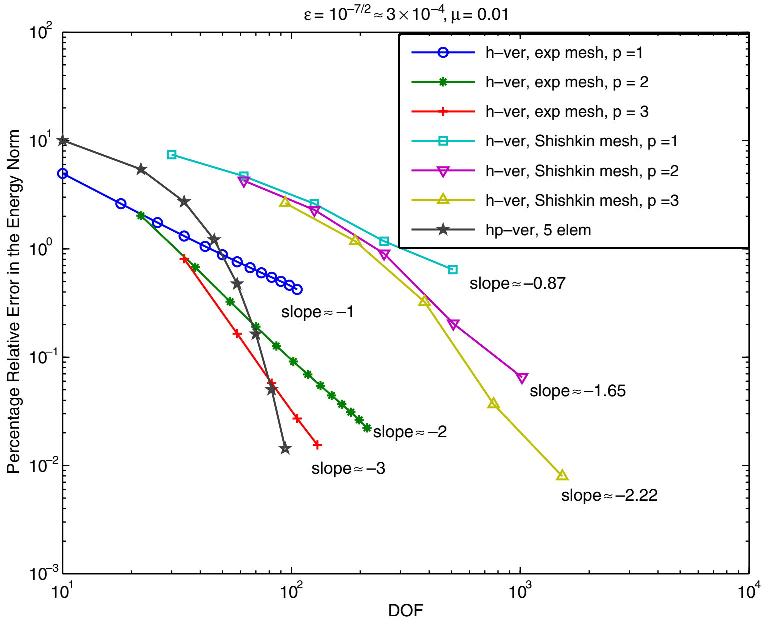


Fig. 8. Energy norm convergence for $\varepsilon = 10^{-7/2} \approx 3 \times 10^{-4}$ and $\mu = 0.01$.

The situation remains the same as $\varepsilon$ and $\mu$ decrease even further, as is shown in Fig. 9, in which $\varepsilon = 10^{-5}$ and $\mu = 10^{-3}$ (smaller values for $\varepsilon$ and $\mu$ produce almost identical results).

We also show, in Fig. 10, the *hp* version on the five element mesh for different values of $\varepsilon$ and $\mu$, and we observe that the method not only does not deteriorate as $\varepsilon, \mu \to 0$, but it actually performs better, when the error is measured in the energy norm. This is reflected by the positive powers of $\varepsilon$ and $\mu$ in the error estimate (21). Although not shown, this behavior is also present in the *h* version on the exponential mesh.

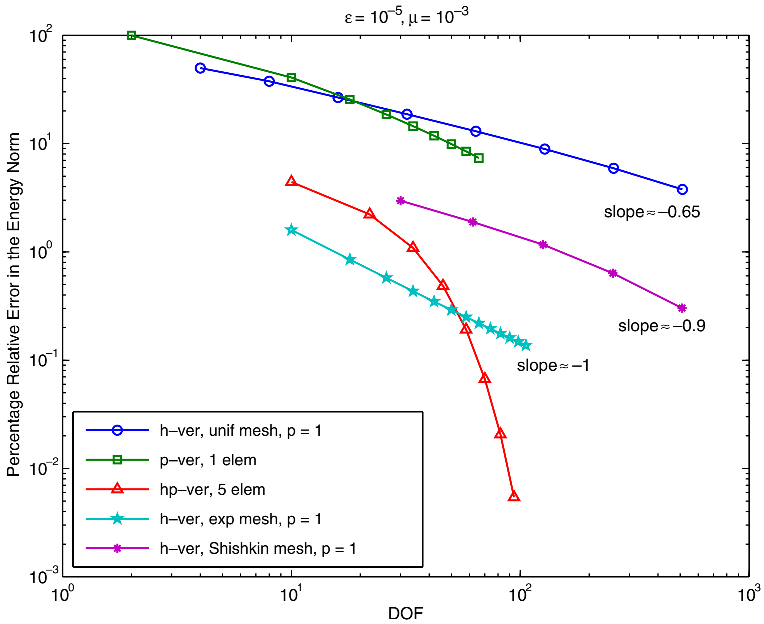


Fig. 9. Energy norm convergence for $\varepsilon = 10^{-5}$ and $\mu = 10^{-3}$.

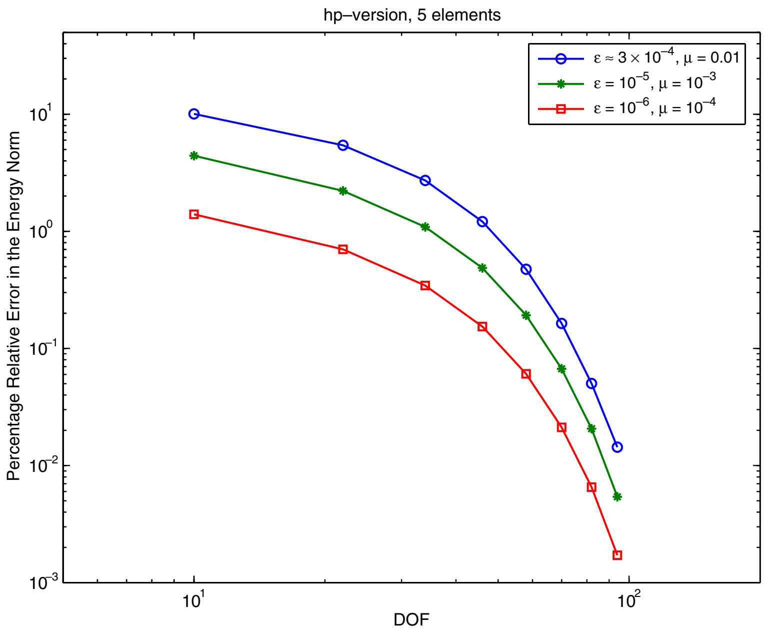


Fig. 10. Energy norm convergence for the *hp* version.

**Remark 1.** Strictly speaking, the *hp* scheme considered here is not a *true hp* FEM, since the position, and not the number of elements, is changing as $p$ is increased. A more accurate characterization of this scheme would be a $p$ version FEM on an appropriately designed (variable) mesh. It is possible, nonetheless, to obtain a true *hp* FEM by using the exponentially graded mesh (or even the Shishkin mesh, as was done in [27] for convection–diffusion problems) in conjunction with increasing $p$. This is shown in Fig. 11, in which we see how the true *hp* version (using the exponential mesh) compares with the one on five elements, in the cases $\varepsilon = 10^{-5}$, $\mu = 10^{-3}$ and $\varepsilon = 10^{-6}$, $\mu = 10^{-4}$.

**Remark 2.** When the maximum norm is used as an error measure, the results are very similar to the ones shown before. Here, for completeness, we show in Fig. 12 a representative plot for the error given by

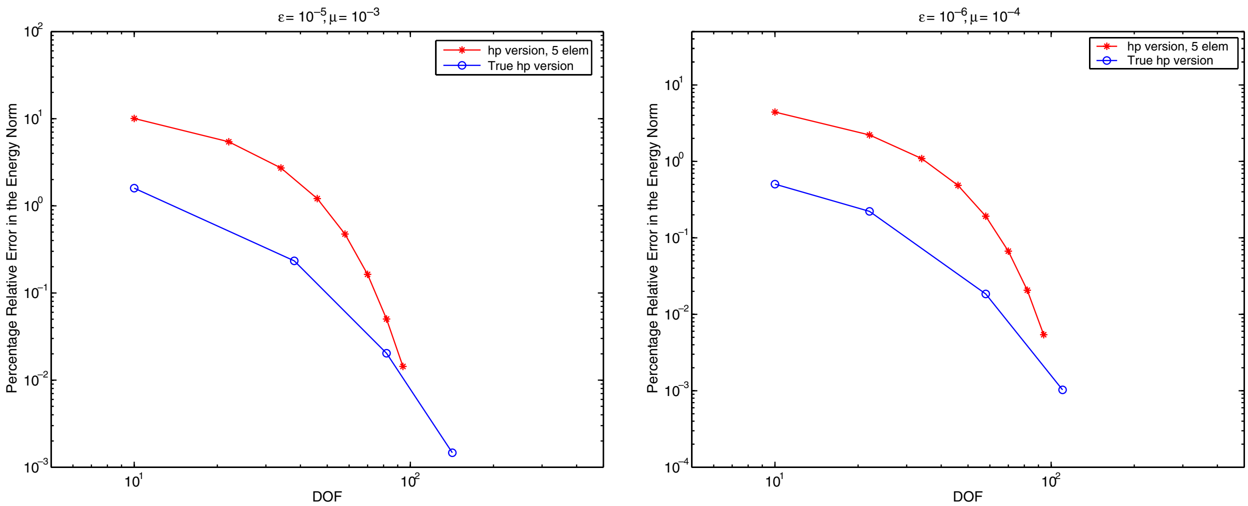


Fig. 11. Energy norm convergence for the *hp* version with five elements and the true *hp* version.

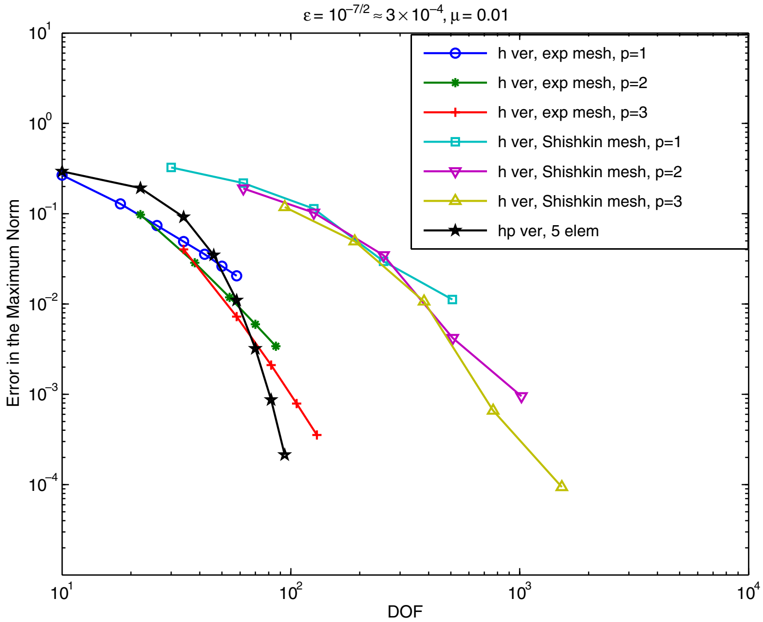


Fig. 12. Maximum norm convergence for $\varepsilon = 10^{-7/2} \approx 3 \times 10^{-4}$ and $\mu = 0.01$.

$$\|\vec{u}_{\mathrm{EXACT}} - \vec{u}_{\mathrm{FEM}}\|_{\infty,\Omega} = \max_{k=1,2} \left\{ \max_{[0,1]} |\vec{u}_{\mathrm{EXACT}} - \vec{u}_{\mathrm{FEM}}| \right\}, \tag{23}$$

versus the number of degrees of freedom, $N$, for the case $\varepsilon = 10^{-7/2} \approx 3 \times 10^{-4}$ and $\mu = 0.01$ (other values of these parameters yield similar results). The slopes of the lines in Fig. 12 are approximately equal to the ones in Fig. 8. It is interesting, but not surprising, to note that when (23) is used as an error measure, the performance of the *hp* version does not improve as $\varepsilon, \mu \to 0$, as was the case when the energy norm was used to measure the error. This is shown in Fig. 13, and is due to the fact that from (21) and the interpolation inequality

$$\|v\|_{\infty,\Omega} \leqslant 2\|v\|_{0,\Omega}^{1/2}\|v'\|_{0,\Omega}^{1/2},$$

one can obtain an error estimate for the error in the maximum norm in which the positive powers of $\varepsilon$ and $\mu$ will not be present (see [26] for more details).

Lastly, we wish to see how the methods perform in the case $\mu = 1$, i.e. when we approximate the solution to the scalar fourth-order singularly perturbed problem studied in [18]. Figs. 14 and 15 show the energy norm convergence plot for the various FEMs, in the cases $\varepsilon = 10^{-3}$, $\mu = 1$ and $\varepsilon = 10^{-4}$, $\mu = 1$, respectively. (For larger values of $\varepsilon$ the *h* version on a uniform mesh and the *p* version on a single element perform reasonably well and the use of a non-uniform refinement is not as crucial, see, e.g., Fig. 4, while for smaller values of $\varepsilon$ the results are similar to the ones shown here.) We should point out that since $\mu = 1$, the *hp* version considered now consists of only three elements (like in the scalar case, cf. (18)).

From these figures we see that the performance of each method does not change significantly when $\mu = 1$, i.e. the *h* version on the uniform mesh and the *p* version on 1 element are not robust, while the *h* version on the Shishkin and exponential meshes, as well as the *hp* version are robust and behave in the same way they did for the values of $\mu$ considered earlier. (The slope of the lines in Figs. 14 and 15 are almost identical to the ones in Fig. 8.) There is, however, one exception: when $p = 1$, the *h* version on the exponential and Shishkin meshes converge at the same rate as it did before but the errors obtained are visibly higher (compare, e.g., Figs. 14 and 15 with Fig. 8). We believe that this is due to the fact that the same (non-uniform) mesh is used for the approximation of both components of $\vec{u} = [u_1(x), u_2(x)]^{\mathrm{T}}$, while $u_2(x)$ is smooth with no boundary layers and a non-uniform mesh may not be the "best" choice. This does not happen when the polynomial degree is $p = 2$ or 3, and we believe that this is due to the better approximation properties that higher order polynomials possess. We do not wish to dwell on this issue, since after all the behavior of all the robust methods is quite satisfactory.

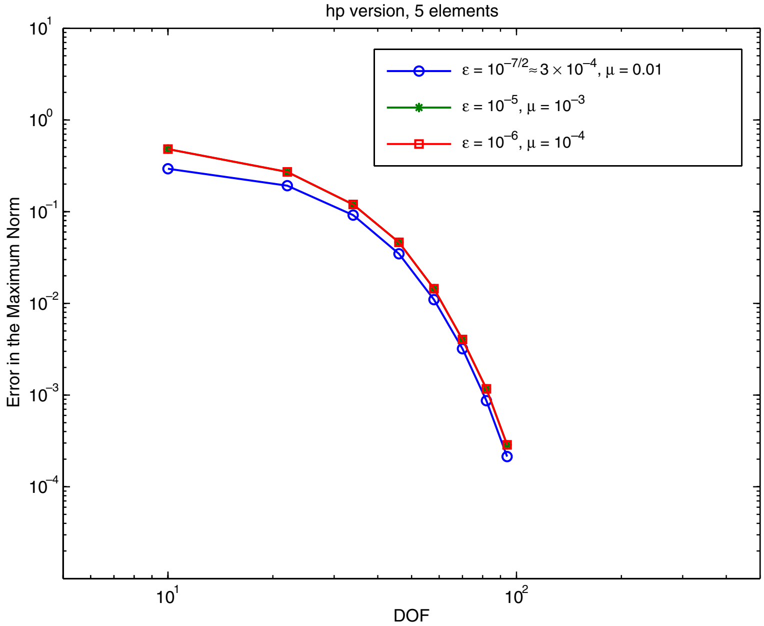


Fig. 13. Maximum norm convergence for the *hp* version.

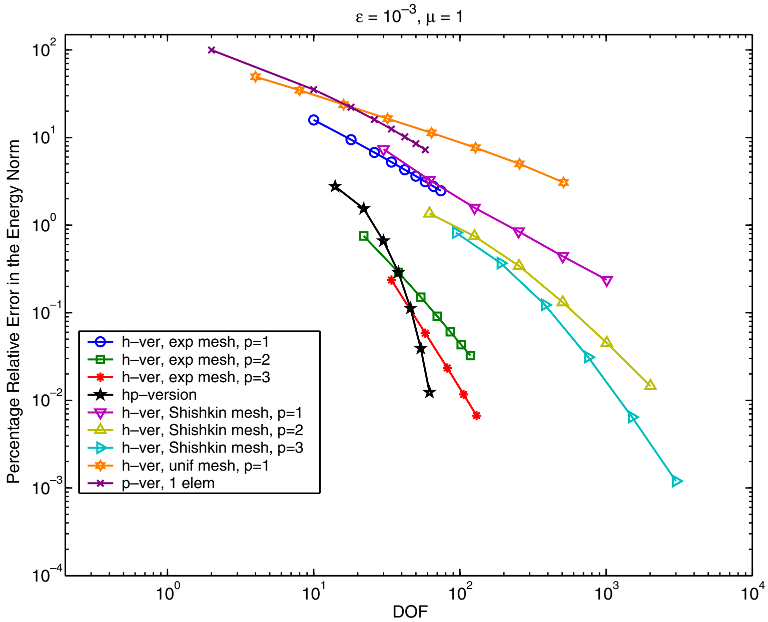


Fig. 14. Energy norm convergence for $\varepsilon = 10^{-3}$ and $\mu = 1$.

## 4.2. The variable coefficient case

Next, we consider the variable coefficient case, in which

$$A = \begin{bmatrix} 2(x+1)^2 & -(1+x^2) \\ -2\cos(\pi x/4) & 2.2e^{1-x} \end{bmatrix}, \quad \vec{f}(x) = \begin{bmatrix} 2e^x \\ 10x+1 \end{bmatrix}, \quad \vec{u}(0) = \begin{bmatrix} 0 \\ 0 \end{bmatrix}.$$

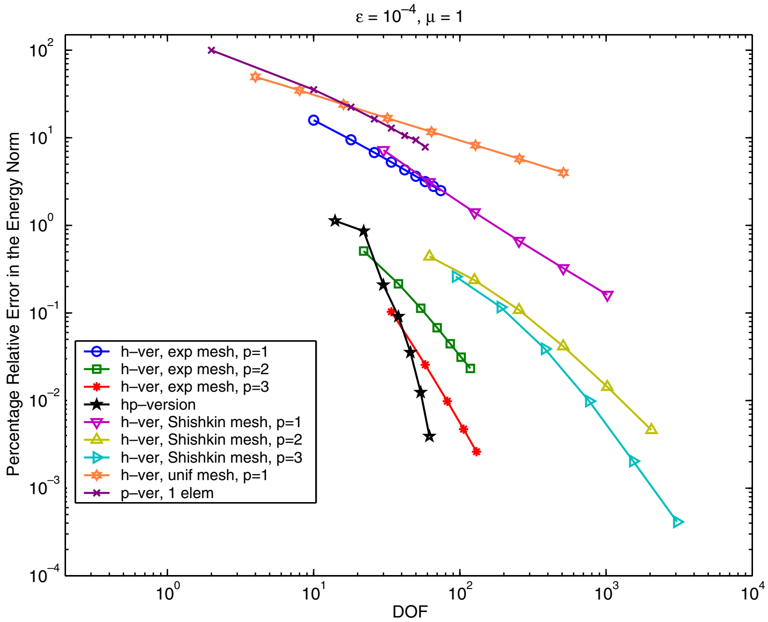


Fig. 15. Energy norm convergence for $\varepsilon = 10^{-4}$ and $\mu = 1$.

An exact solution is not available, and for our computations we use a reference solution obtained with polynomials of degree 8 on the exponentially graded mesh (19), supplemented with a uniform refinement of $N/3$ elements in the middle of the domain (see Fig. 16). Since this is a variable coefficient problem with non-constant right-hand side, the addition of the uniform refinement is necessary in order for all the components of the solution to be accurately approximated. Hence, in our computations we add this uniform refinement to the exponential mesh as well, and we refer to it as a "modified exponential mesh".

We are again interested in the (now estimated) percentage relative error in the energy and maximum norms. However, given the results obtained for the constant coefficient case, we now focus our attention only on the methods which converge uniformly in $\varepsilon$ and $\mu$, namely

- The *hp* version on the five element (variable) mesh given by (20).
- The *h* version on a Shishkin mesh, with $p = 1$, 2 and 3.
- The *h* version on the modified exponential mesh, with $p = 1$, 2 and 3.

Figs. 17 and 18 show the energy norm convergence of the above three methods for $\varepsilon = 10^{-7/2} \approx 3 \times 10^{-4}$, $\mu = 0.01$ and $\varepsilon = 10^{-5}$, $\mu = 10^{-3}$, respectively. The results are almost identical to the constant coefficient case and they indicate, once more, the robust algebraic convergence rates for the *h* versions and the exponential convergence rate for the *hp* version.

In Fig. 19 we show the *hp* version on the five element mesh, for different values of $\varepsilon$ and $\mu$, and we observe that the positive powers of $\varepsilon$ and $\mu$ in the error estimate (21) are present in the variable coefficient case as well, when the error is measured in the energy norm.

The performance of the robust FEMs when the error is measured in the maximum norm is shown in Fig. 20, which corresponds to $\varepsilon = 10^{-6}$ and $\mu = 10^{-4}$. As in the constant coefficient case, the situation does

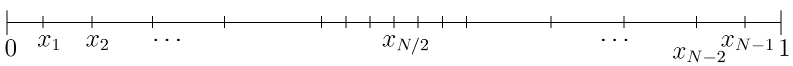

Fig. 16. Modified exponential mesh.

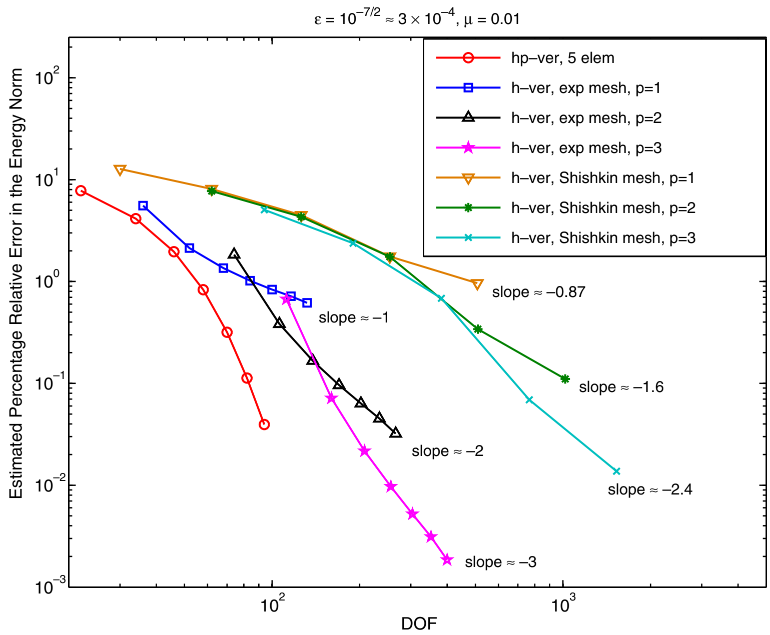


Fig. 17. Energy norm convergence for $\varepsilon = 10^{-7/2} \approx 3 \times 10^{-4}$ and $\mu = 0.01$.

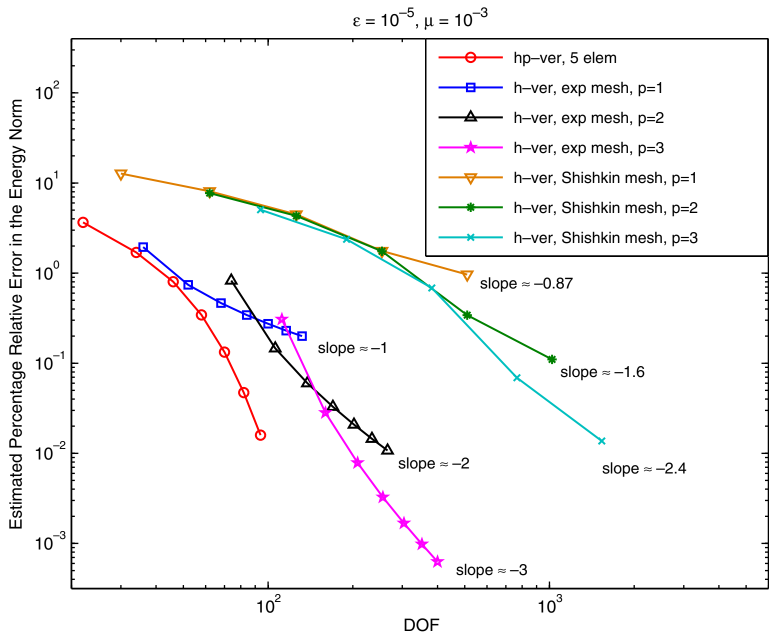


Fig. 18. Energy norm convergence for $\varepsilon = 10^{-5}$ and $\mu = 10^{-3}$.

not change with the error measure, and all of the observations made in the previous subsection carry over to the variable coefficient case.

Finally, we consider the cases $\varepsilon = 10^{-3}$, $\mu = 1$ and $\varepsilon = 10^{-4}$, $\mu = 1$, which correspond to the scalar fourth-order singularly perturbed problem [18]. Figs. 21 and 22 show the performance of the robust methods: the results are almost identical as in the previous example, and qualitatively the same as all other values of $\varepsilon$ and $\mu$ we have considered in this work.

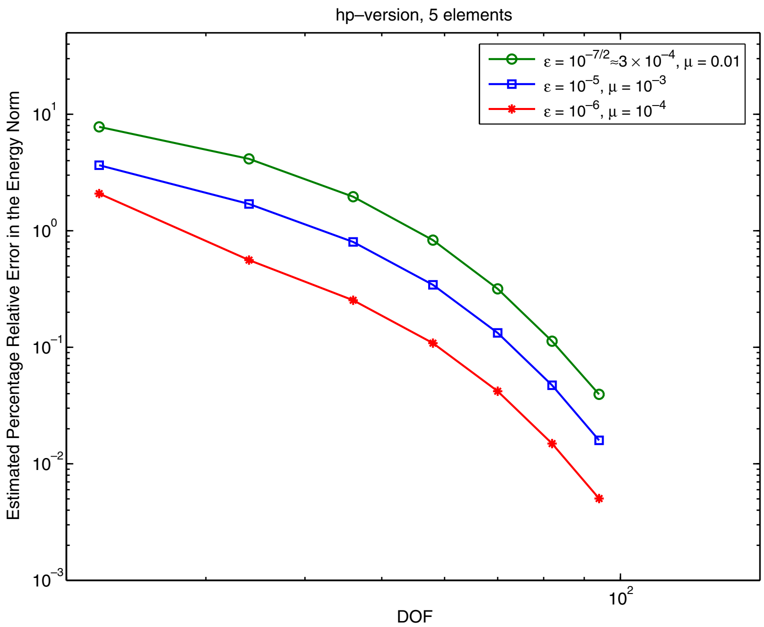


Fig. 19. Energy norm convergence for the *hp* version.

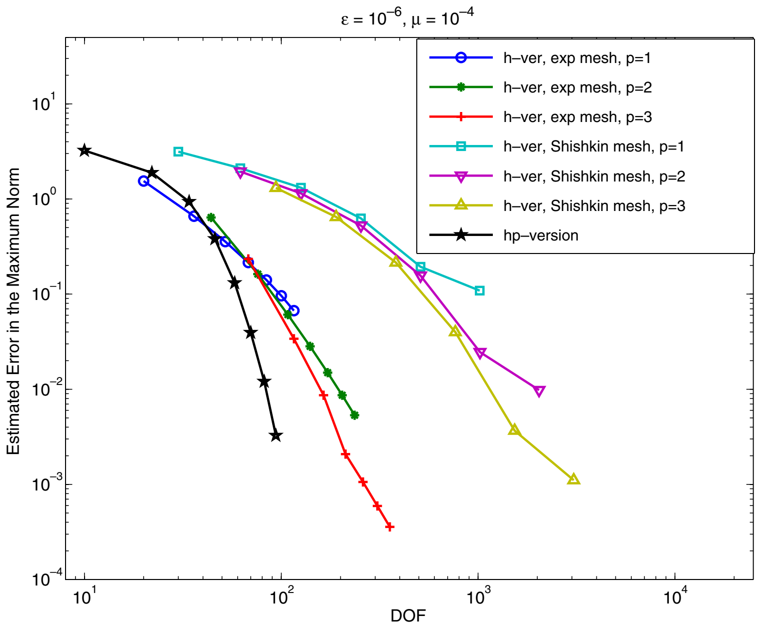


Fig. 20. Maximum norm convergence for $\varepsilon = 10^{-6}$ and $\mu = 10^{-4}$.

## 5. Conclusions

We have studied the finite element approximation of systems of singularly perturbed reaction–diffusion problems by various versions of the FEM. For the model problem under consideration, we have demonstrated numerically how the $h$ version on a uniform mesh and the $p$ version on a single element do not converge uniformly, as $\varepsilon, \mu \to 0$, while the $h$ version on either a Shishkin or an exponentially graded mesh, is robust and its

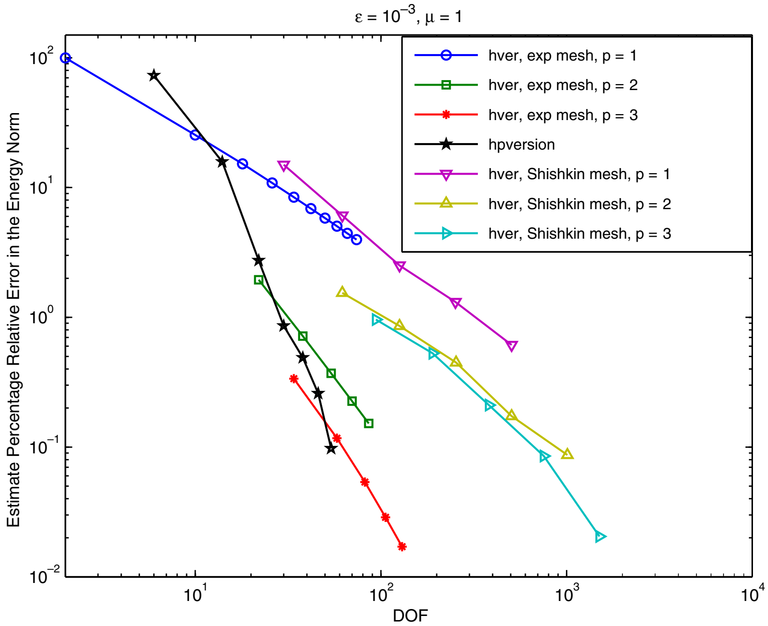


Fig. 21. Energy norm convergence for $\varepsilon = 10^{-3}$ and $\mu = 1$.

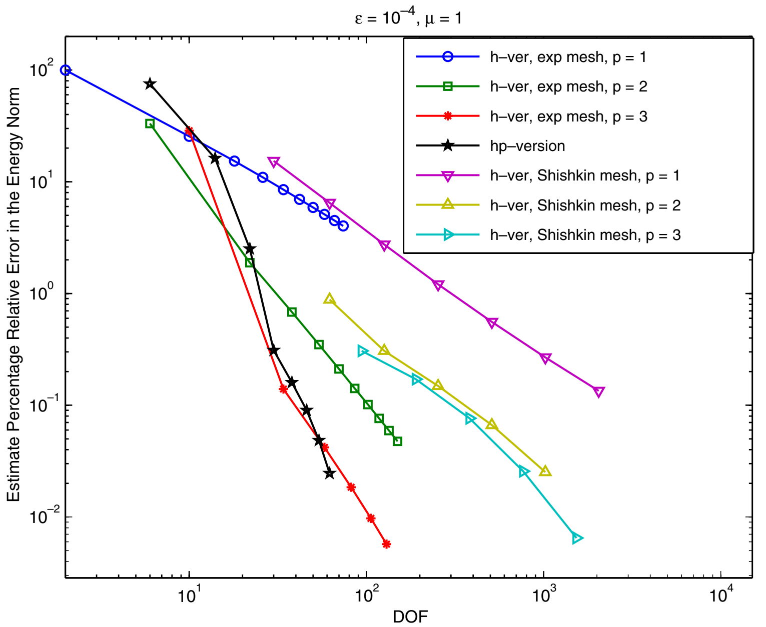


Fig. 22. Energy norm convergence for $\varepsilon = 10^{-4}$ and $\mu = 1$.

performance does not deteriorate as $\varepsilon, \mu \to 0$. In particular, when the $h$ version is used with polynomials of degree $p$ on a Shishkin mesh, we observe $O((N^{-1}\ln N)^p)$ convergence, and when the same method is used on the exponentially graded mesh, the logarithmic term is no longer present and the optimal $O(N^{-p})$ convergence rate is observed. We also proposed an $hp$ scheme on a five element variable mesh which converges uniformly in $\varepsilon$ and $\mu$ at an exponential rate.

The above remarks are valid when the error is measured in the energy and maximum norms, and for the range of values $0 < \varepsilon \leqslant \mu \leqslant 1$, including the case $\mu = 1$ which corresponds to the scalar fourth-order singularly perturbed problem.

The numerical analysis of the proposed *hp* scheme, and the proof of the observed exponential rate of convergence is carried out in [26].

## References

[1] N.S. Bakhvalov, Towards optimization of methods for solving boundary value problems in the presence of boundary layers, Zh. Vychisl. Mat. Mat. Fiz. 9 (1969) 841–859 (in Russian).
[2] I.A. Blatov, On the Galerkin finite-element method for elliptic quasilinear singularly perturbed boundary value problems I, Differen. Eqs. 28 (1993) 931–940.
[3] I.A. Blatov, On the Galerkin finite-element method for elliptic quasilinear singularly perturbed boundary value problems II, Differen. Eqs. 28 (1993) 1469–1477.
[4] G. Beckett, J.A. Mackenzie, Uniformly convergent high order finite element solutions for a singularly perturbed reaction–diffusion equation using mesh equidistribution, Appl. Numer. Math. 39 (2001) 31–45.
[5] Y. Kan-On, M. Mimura, Singular perturbation approach to a 3-component reaction–diffusion system arising in population dynamics, SIAM J. Math. Anal. 29 (1998) 1519–1536.
[6] J. Li, Convergence and superconvergence analysis of finite element methods on highly nonuniform anisotropic meshes for singularly perturbed reaction–diffusion problems, Appl. Numer. Math. 36 (2001) 129–154.
[7] T. Linß, N. Madden, A finite element analysis of a coupled system of singularly perturbed reaction–diffusion equations, Appl. Math. Comput. 148 (2004) 869–880.
[8] T. Linß, N. Madden, An improved error estimate for a numerical method for a system of coupled singularly perturbed reaction–diffusion equations, Comput. Methods Appl. Math. 3 (2003) 417–423.
[9] T. Linß, N. Madden, Accurate solution of a system of coupled singularly perturbed reaction–diffusion equations, Computing 73 (2004) 121–133.
[10] N. Madden, M. Stynes, A uniformly convergent numerical method for a coupled system of two singularly perturbed linear reaction–diffusion problems, IMA J. Numer. Anal. 23 (2003) 627–644.
[11] S. Matthews, E. O'Riordan, G.I. Shishkin, A numerical method for a system of singularly perturbed reaction–diffusion equations, J. Comput. Appl. Math. 145 (2002) 151–166.
[12] S. Matthews, J.J.H. Miller, E. O'Riordan, G.I. Shishkin, A parameter robust numerical method for a system of singularly perturbed ordinary differential equations, in: J.J.H. Miller, G.I. Shishkin, L. Vulkov (Eds.), Analytical and Numerical Methods for Convection-dominated and Singularly Perturbed Problems, Nova Science Publishers, New York, 2000, pp. 219–224.
[13] M.J. Melenk, On the robust exponential convergence of *hp* finite element method for problems with boundary layers, IMA J. Numer. Anal. 17 (1997) 577–601.
[14] J.J.H. Miller, E. O'Riordan, G.I. Shishkin, Fitted Numerical Methods Singular Perturbation Problems, World Scientific, 1996.
[15] K.W. Morton, Numerical solution of convection–diffusion problems, Applied Mathematics and Mathematical Computation, vol. 12, Chapman & Hall, 1996.
[16] W. Rodi, Turbulence Models and their Applications in Hydraulics, in: IAHR Monograph Series, A.A. Balkema, Rotterdam, 1993.
[17] H.G. Roos, M. Stynes, L. Tobiska, Numerical methods for singularly perturbed differential equations, Springer Series in Computational Mathematics, vol. 24, Springer Verlag, 1996.
[18] V. Santhi, N. Ramanujan, A numerical method for boundary value problems for singularly perturbed fourth-order ordinary differential equations, Appl. Math. Comput. 129 (2002) 269–294.
[19] G.I. Shishkin, Mesh approximation of singularly perturbed boundary value problems for systems of elliptic and parabolic equations, Comput. Methods Math. Phys. 35 (1995) 429–446.
[20] G.I. Shishkin, Grid approximation of singularly perturbed boundary value problems with a regular boundary layer, Sov. J. Numer. Anal. Math. Model. 4 (1989) 397–417.
[21] C. Schwab, M. Suri, The *p* and *hp* versions of the finite element method for problems with boundary layers, Math. Comput. 65 (1996) 1403–1429.
[22] G.P. Thomas, Towards an improved turbulence model for wave-current interactions, 2nd Annual Report to EU MAST-III Project The Kinematics and Dynamics of Wave-Current Interactions, Contract No MAS3-CT95-0011, 1998.
[23] C. Xenophontos, The hp finite element method for singularly perturbed problems, Ph.D. Dissertation, University of Maryland, 1996.
[24] C. Xenophontos, Optimal mesh design for the finite element approximation of reaction–diffusion problems, Int. J. Numer. Methods Eng. 53 (2002) 929–943.
[25] C. Xenophontos, A note on the convergence rate of the finite element method for singularly perturbed problems using the Shishkin mesh, Appl. Math. Comput. 142 (2003) 545–559.
[26] C. Xenophontos, L. Oberbroeckling, An *hp* finite element method for singularly perturbed systems of reaction–diffusion problems, in preparation.
[27] Z. Zhang, On the *hp* finite element method for the one dimensional singularly perturbed convection–diffusion problems, J. Comput. Math. 20 (2002) 599–610.